Antiviral Research 212 (2023) 105554

Contents lists available at ScienceDirect

Antiviral Research

journal homepage: www.elsevier.com/locate/antiviral

Ebola virus disease: *In vivo* protection provided by the PAMP restricted TLR3 agonist rintatolimod and its mechanism of action

Angela Corona [a], David Strayer [b], Simona Distinto [a], Gian Luca Daino [a], Annalaura Paulis [a], Enzo Tramontano [a], William M. Mitchell [c,*]

[a] Department of Life and Environmental Sciences, University of Cagliari, 09042, Monserrato, Italy
[b] AIM ImmunoTech, Ocala, FL, 34473, USA
[c] Vanderbilt University, Vanderbilt University School of Medicine, C-3321 MCN Dept. of Pathology, Microbiology and Immunology, Nashville, TN, 37232, USA

ARTICLE INFO

Keywords:
Ebola virus (EBOV)
VP35
EBOV Lethal factor
Type I Interferons
Rintatolimod (Ampligen)
PAMP-Restricted TLR3 agonist

ABSTRACT

Ebola virus (EBOV) is a highly infectious and lethal pathogen responsible for sporadic self-limiting clusters of Ebola virus disease (EVD) in Central Africa capable of reaching epidemic status. 100% protection from lethal EBOV-Zaire in Balb/c mice was achieved by rintatolimod (Ampligen) at the well tolerated human clinical dose of 6 mg/kg. The data indicate that the mechanism of action is rintatolimod's dual ability to act as both a competitive decoy for the IID domain of VP35 blocking viral dsRNA sequestration and as a pathogen-associated molecular pattern (PAMP) restricted agonist for direct TLR3 activation but lacking RIG-1-like cytosolic helicase agonist properties. These data show promise for rintatolimod as a prophylactic therapy against human Ebola outbreaks.

1. Introduction

Ebola virus (EBOV) is a highly infectious and pathogenic member of the Filoviridae family of filamentous single-stranded RNA viruses responsible for sporadic clusters of Ebola virus disease (EVD) in Central Africa capable of reaching epidemic status (Feldmann et al., 2013). The largest epidemic to date occurred in 2014–2016 in West Africa with more than 11,000 deaths (CDC, 2016). In 2021 two new outbreaks occurred in the Democratic Republic of the Congo and Guinea (Adepolu, 2021). Next generation sequencing of EBOV has suggested persistence of prior infection and latency with activation and lateral spread (Keita et al., 2021). Most recently a Sudan EBOV outbreak occurred in Uganda in 2022–23 (WHO, 2023).

Death from EBOV infection is associated with markedly impaired coagulation cascades, suppressed innate immune responses to the infection, increased production of pro-inflammatory cytokines, profound immune suppression resulting in peripheral T lymphocyte apoptosis and delayed adaptive immunity. Survivors of EVD develop an effective immune response with the production of EBOV neutralizing antibodies. Disarming innate immune responses by interference with essential interferon (IFN) production, as well as the multiplicity of IFN stimulated genes (ISG), is a common method employed by highly pathogenic human viruses (García-Sastre, 2017). A key point of EBOV pathogenesis is the efficient evasion of the innate immune interference against the infection (Mahanty and Bray, 2004). In particular, two viral proteins, VP35 and VP24, block type-1 IFN production and signaling, respectively, provoking a rapid impairment of the cellular innate immune defense machinery and are attractive targets for drug development (Fanunza et al., 2019). The VP35 multifunctional protein is an essential component of EBOV replication and it potently inhibits RIG-I-like cytosolic helicase receptor(s) (RLR) signaling in an homo-dimeric form essential for its activity (Di Palma et al., 2019; Zinzula et al., 2019, 2022). The EBOV VP35 IFN inhibitory domain (IID) is the region involved in the evasion of the IFN response, being responsible for VP35-viral dsRNA binding, preventing its recognition by RIG-I (Fanunza et al., 2018a; Paulis et al., 2021; Zinzula and Tramontano, 2013). Previous studies revealed that mutation of key basic residues within the IID results in significant EBOV attenuation, with

Abbreviations: EBOV, Ebola virus; EVD, Ebola virus disease; maEBOV, mouse adapted Ebola virus; EBOV- Zaire, Ebola virus Zaire strain; dsRNA, double stranded RNA; pfu, plaque forming units; ISG, interferon stimulated genes; VP35, lethal factor 35K mw viral protein; IID, VP35 IFN inhibitory domain; PAMP, pathogen associated molecular pattern; USAMRIID, United States Army Medical Research Institute of Infectious Diseases; PDB, Protein Data Bank.

* Corresponding author.
E-mail address: bill.mitchell@vanderbilt.edu (W.M. Mitchell).

https://doi.org/10.1016/j.antiviral.2023.105554
Received 22 November 2022; Received in revised form 30 January 2023; Accepted 6 February 2023
Available online 16 February 2023

diminished, or abolished suppression of IFN-β induction, validating it as a drug target (Prins et al., 2009, 2010).

EBOV VP35 is critical for virulence in non-human primates (Woolsey et al., 2019). EBOV variants carrying mutations in VP35 residues critical for innate immune evasion do not cause lethal disease in primates and instead elicit adaptive immune responses that can protect animals from wild-type EBOV challenge (Seesuay et al., 2018).

Two drugs are approved currently for EVD treatments. Inmazeb is a combination of three monoclonal antibodies. Ebanga is a single monoclonal antibody. Given the limits in the use of monoclonal antibodies, new drugs are needed to face possible new EBOV epidemics. Recent reports indicate that molecules able to counteract VP35 inhibition of innate immune response can block EBOV replication in cell-based assays (Corona et al., 2022). Following an alternative approach, in this report we demonstrate 90–100% protection from 100% lethal EBOV challenge in a mouse model of EVD with the PAMP-restricted TLR3 agonist, rintatolimod (Ampligen). Rintatolimod is a mismatched double-stranded (ds) RNA (poly I:poly $C_{12}U$) with PAMP activity restricted to the transient activation of TLR3 (Gowen et al., 2007; Trumpfheller et al., 2008) and the derivative interferon stimulated genes (ISG) 2′-5′ adenylate synthetase (Hartmann et al., 2003) and protein kinase R (Lemaire et al., 2008), which require ds RNA for activation. We also investigated rintatolimod's mechanism of protection demonstrating that it is provided by both rintatolimod's activation of the TLR3 innate immune responsses and inhibition of EBOV VP35 function to suppress innate immune responses to infection.

2. Methods

2.1. In vivo efficacy

Rintatolimod was evaluated in female BALB/c mice (10/group) at the United States Army Medical Research Institute of Infectious Diseases (USAMRIID, Ft. Detrick, MD) under BSL4 conditions by a method developed at USAMRIID for its routine evaluation of potential human therapeutics for EVD (Bray et al., 1998). The mouse model closely resembles the pathogenesis of more laborious and costly infectious EBOV models in guinea pigs and nonhuman primates (Gibb et al., 2001). BALB/c mice were infected with 1000 pfu of mouse-adapted EBOV given intraperitoneal (IP) and 4 h later treated with IP rintatolimod (0, 6, 12, or 18 mg/kg) every other day with the last dose of rintatolimod given on Day 12. Mice were observed for weight and survival for 21 days post-infection. Weight represents the group weight of all surviving animals in each dosage group.

The USAMRIID protocol uses 8 week old female mice housed in filter-top micro-isolation cages with commercial mouse feed and fresh water ad libitum. The mouse adapted EBOV- Zaire has a LD_{50} of ~1 virion (1/30th pfu in Vero cells) when administered IP (Bray et al., 1998).

2.2. dsRNA binding to ebola VP35

EBOV VP35 binding assays were performed using a recombinant VP35 (rVP35) and conditions previously described (Zinzula et al., 2009, 2012). Briefly, a heterologous tritium labeled ^{3}H-cytidine monophosphate (500 bp 5′-triphosphate capped dsRNA) was used to quantify rintatolimod inhibition of binding to a rVP35 at 20 mM $MgCl_2$ using an immobilized rVP35 His-tag magnetic pull-down procedure to quantify bound dsRNA.

Rintatolimod (Lot #0702HE) is a clinical grade Poly I:Poly $C_{12}U$ polymer with a weight average MW of 845,700 Da (845.7 kdaltons) with ~1264 bp/dsRNA (the general release specifications for clinical grade rintatolimod are provided in Supplementary Table S1).

An unlabeled triphosphate-dsRNA of 8 bp was used as positive control for labeled dsRNA displacement. The data were plotted as the mean ± SD of the average of two independent in duplicate experiments using GraphPad Prism.

2.3. HEK-Blue hTLR3 Cell IFN-beta reporter assay

HEK-Blue hTLR3 cells are HEK-Blue Null1 cells (InvivoGen) stably transfected with human TLR3, which expresses a secreted embryonic alkaline phosphatase (SEAP) reporter gene under the control of the IFN-β minimal promoter fused to five NF-κB and AP-1 binding sites. Cell growth medium consisted of DMEM, 4.5 g/l glucose (Gibco), 10% (v/v) fetal bovine serum (FBS) (Gibco), 100 U/ml penicillin (Gibco), 100 mg/ml streptomycin(Gibco), 100 mg/ml Normocin (InvivoGen) and 2 mM L-glutamine (Gibco). The HEK-Blue Null1 cell medium contained 100 μg/ml Zeocin (InvivoGen). The HEK-Blue hTLR3 cell medium contained 30 μg/ml of blasticidin (InvivoGen) and 100 μg/ml of Zeocin (InvivoGen). 10 mL containing various concentrations of rintatolimod pre-incubated for 15 min in serum free Opti-MEM (Gibco) with 4% Lipofectamine (Thermo Fisher Scientific) was added to HEK-Blue Null1 (Invivogen) or HEK-Blue hTLR3 (Invivogen) cells at ~280,000 cells per ml in HEK-Bluedetection medium (Invivogen), mixed, and aliquoted at ~25,000 cells per well in transparent 96 microwell plates and incubated at 37 °C in 5% CO_2 for 24 h. Alkaline phosphatase was quantified colorimetrically using a Viktor Nivo 5 plate reader at 620 nm.

2.4. Gene reporter assay

The Luciferase Reporter Gene Assay was adapted from Fanunza et al. and Cannas et al. (Cannas et al., 2015; Fanunza et al., 2018b) HEK293T Cells (~1.5×10^4 cells/well) were seeded in 96-well plates 24 h before transfection. Cells were transfected using T-Pro P-Fect III Transfection Reagent (T-Pro Biotechnology), according to the manufacturer's protocol. Plasmids (pGL–IFN–β-luc 60 ng; pRL-TK 10 ng plus various dilutions of pcDNA3 (InvivoGen) as an empty vector (EV) control or pVP35 (obtained as reported by Cannas et al. (2015) were mixed with the transfection reagent in reduced serum medium Opti-MEM (Gibco) and incubated 20 min at room temperature. Transfection complexes were then gently added into individual wells of the 96-well plate. Twenty-four hours after transfection, cells were stimulated with influenza virus RNA (IAV-RNA) with various rintatolimod doses pre-mixed with the transfection reagent in reduced serum medium Opti-MEM and incubated for 24 h at 37 °C in 5% CO_2. Cells were harvested with lysis buffer (50 mM Na-MES [pH 7.8], 50 mM Tris-HCl [pH 7.8], 1 mM dithiothreitol, and 0.2% Triton X-100) (Merck). To lysates were added luciferase assay buffer (125 mM Na-MES [pH 7.8], 125 mM Tris-HCl [pH 7.8], 25 mM magnesium acetate, and 2.5 mg/mL ATP) (Merck). Immediately after addition of 50 μl of Luciferin buffer (25 mM D-luciferin (GoldBio), 5 mM KH_2PO_4) the luminescence was measured in a Victor 3 luminometer (PerkinElmer), and again after addition of 50 μl of Coelenterazine assay buffer (125 mM Na-MES [pH 7.8], 125 mM Tris-HCl [pH 7.8], 25 mM magnesium acetate, 5 mM KH_2PO_4 and 10 μM Coelenterazine (Santa Cruz Biotechnology). The relative light units (RLU) of Luciferase signal were normalized to Renilla Luc vs unstimulated controls. Each assay was performed in triplicate. Results were expressed in percentage of IFN induction, analyzed as a *t*-test vs the EV control (indicated as 100%). The data were plotted as the mean ± SD of the average of two independent experiments using GraphPad Prism 9.01 for statistical analysis. P-values were calculated by unpaired, two-tailed t-tests (GraphPad Prism 9.01).

2.5. qPCR assay

HEK293T Cells (3×10^5 cells/well), resuspended in Dulbecco's modified Eagle's medium (MEM) supplemented with 10% fetal bovine serum (FBS), were seeded in 6-well plates, pre-treated with 500 μl of Poly-D-lysine hydrobromide (Merck) (100 μg/ml) for 1 h. After 24 h, 2500 ng of plasmid pcDNA3 for empty vector (EV) controls or pcDNA3 VP35 expressing VP35 were used to transfect the HEK293T cells with Lipofectamine 3000 (InvivoGen) according to the manufacturer's

protocol. Twenty-four hours after transfection, cells were stimulated with 2500 ng of IAV-RNA with or without rintatolimod, pre-mixed with the transfection reagent in reduced serum medium Opti-MEM (Gibco), and incubated for 24 h at 37 °C under 5% CO_2. Total RNA was extracted from transfected cells with TRIzol (Invitrogen). RNA was then reverse transcribed and amplified using Luna Universal One-Step RT-qPCR kit (New England Biolabs). Quantitative real time PCR (RT-qPCR) was performed in triplicate in a CFX-96 Real-Time system (Biorad). Primers used:

GAPDH Forward 5′-GAGTCAACGGATTTTGGTCGT-3′,
GAPDH Reverse 5′-TTGATTTTGGAGGGATCTCG-3′,
IFN-beta Forward 5′-CTTGGATTCCTACAAAGAAGCAGC-3′,
IFN-beta Reverse 5′- TCCTCCTTCTGGAACTGCTGCA-3’.

Data were analyzed with Opticon Monitor 3.1. mRNA expression levels were normalized to glyceraldehyde-3-phosphate dehydrogenase (GAPDH) levels. Results were expressed as gene copy number or as percentage of gene expression over the empty vector (indicated as 100%) and plotted as mean ± SD of two or more replicate averages with GraphPad Prism 8.0.

2.6. Docking evaluation

The IID of VP35 is located at the C- terminus and distinct in location from its replication function at the N-terminus. The IID (221–340) VP35 coordinates were obtained from the Protein Data Bank (PDB) with code 3L25 (Leung et al., 2010). The docking protocol was validated by re-docking the 8 bp dsRNA with ZDock software (Pierce et al., 2011, 2014) and applying two versions, 3.0.2 and 2.3.2, that differ from the scoring function:

- ZDOCK 3.0.2: IFACE Statistical Potential, Shape Complementarity, and Electrostatics,
- ZDOCK 2.3.2: ACE Statistical Potential, Shape Complementarity, and Electrostatics

The best poses of 3.0.2 had RMSD of 2.1, confirming that this protocol was able to reproduce experimental data reported by Leung and coworkers. Therefore, the same protocol was applied to dock the terminal 8 bp polyI:C structure of rintatolimod dsRNA (Klosterman et al., 1999). The 3D structure of polyI:C was obtained from 1QCU reporting polyG:C dsRNA by removing the amino group in position 2 of guanine bases to obtain the hypoxanthine bases. Then, the polyI:C-dsRNA was docked applying ZDock protocol previously validated. The Protein-Ligand Interaction Profiler (Adasme et al., 2021) was used to examine the non-covalent interactions of the VP35 dsRNA complexes.

2.7. Statistical analysis

Experimental P-values were calculated by unpaired, two-tailed t-tests (GraphPad Prism 9.01).

3. Results

3.1. EBOV mouse challenge

The established mouse model for EBOV infection was 100% lethal for the untreated animals. Fig. 1A demonstrates an average survival of ~5 days (4–6 day range). Rintatolimod treatment by IP initiated 4 h after infection was repeated every other day terminating on day 12 with observation for a total of 21 days (9 untreated days). 100% survival was observed at the lowest dose (6 mg/ml). The average survival for all dosage levels was 93%. Associated with the high survival at the 6 mg/kg dose was weight maintenance throughout the observational period of 21 days (Fig. 1B) and minimal weight loss in the 90% survival groups suggesting that lower levels of survival and weight loss at higher doses of rintatolimod may be secondary to toxicity. Rodents are known to exhibit acute toxicity to rintatolimod that is a magnitude higher than primates (Mitchell et al., 2014).

Prior to animal experimentation the efficacy of rintatolimod *in vitro* was established in a standard virus infectivity assay (Supplementary Fig. S1).

3.2. Mechanism of rintatolimod effect on EBOV VP35

Virulence of EBOV is generally ascribed to sequestration of viral dsRNAs by VP35 inhibiting Type I IFN responses triggered by RIG-like cytosolic helicases (Zinzula et al., 2012). Our hypothesis forming the rationale for our subsequent experimentation is whether PAMP rintatolimod could have an effect on VP35 inhibition of the IFN-production in cell-based assays providing an evidence based mechanism for its efficacy in the mouse model of EBOV infection.

3.2.1. Rintatolimod inhibition of VP35 binding to dsRNA

Initially, we tested the *in vitro* effect of rintatolimod on full length rVP35 binding to dsRNA and observed that it efficiently competes with dsRNA for EBOV rVP35 binding (Fig. 2A) with an IC_{50} value of 1.30 ± 0.21 nM. An unlabeled 8 bp dsRNA was used as positive control for competition with VP35 dsRNA binding (Fig. 2B), that was able to reduce VP35 dsRNA binding with an IC_{50} value of 154 ± 7 nM. Compared to the 8 bp control (Fig. 2B), rintatolimod was approximately 100x more efficient in VP35 inhibition. Note, however, that one molecule of rintatolimod potentially can laterally bind multiple VP35 molecules as

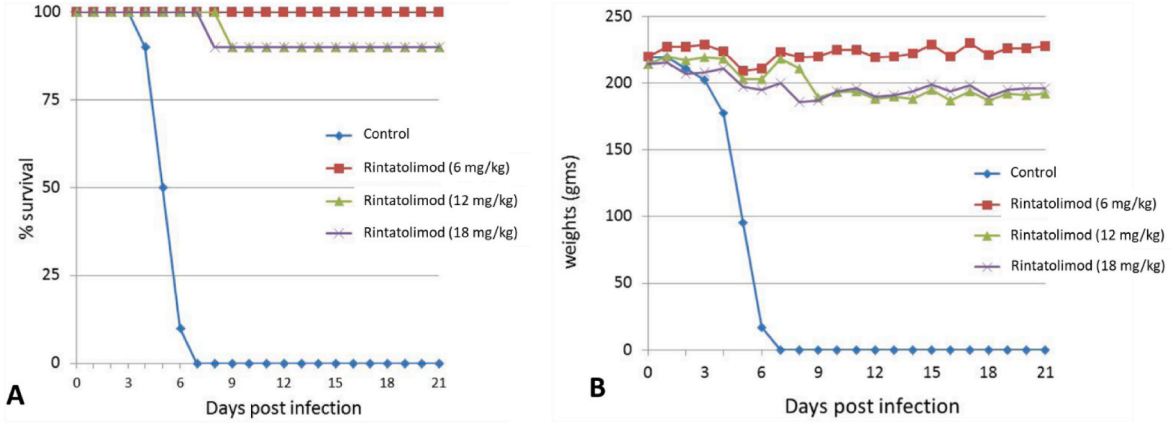

Fig. 1. Rintatolimod effects in Balb/C mice following infection with Ebola virus Zaire. A. Survival data over 21 days observation. B. Weight maintenance as a function of treatment.

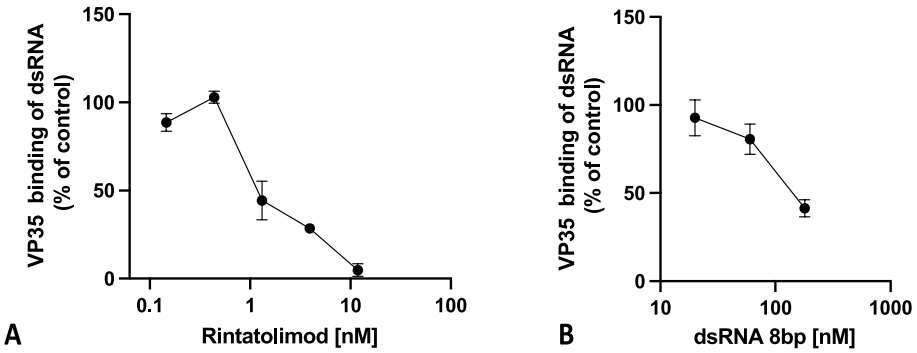

Fig. 2. Inhibition of EBOV rVP35 binding to dsRNA by rintatolimod. A. Inhibition of a 500 bp [^{3}H]triphosphate dsRNA binding to VP35 by rintatolimod. B. Inhibition of 500 bp ^{3}H tri-phosphate dsRNA binding to VP35 by a triphosphate 8 bp dsRNA.

observed with TLR3 (Leonard et al., 2008; Luo et al., 2012) affecting the IC_{50} calculation. Docking experiments were carried out to identify residues predicted to be involved in the binding of polyI:C with VP35 IID. In particular, the phosphate moieties of terminal I_{11}:C_{12} were shown to interact with the end-capping portion of the charge residues K282, R322, K309, the bases with F239, C275, I278, Q279, I340, and the sugar with S272. Overall, the end-capping residues involved in the complex dsRNA (pdb code 3L25) and the docked rintatolimod are the same, but the total number of hydrogen bonds that stabilize the complex VP35-rintatolimod is greater. More backbone-binding residues (chain A) are involved, including S272, K309, P233, S310, R312, and Q274 (Supplementary Table S2, and Fig. S3). Fig. 3 depicts docking in A and B chain asymmetric homodimers. Alignment with other VP35 IID EBOV sequences available in the Uniprot KB databas shows that the binding region and many interacting residues are conserved (Supplementary Fig. S4). As a result, rintatolimod may be effective on these as well. The large

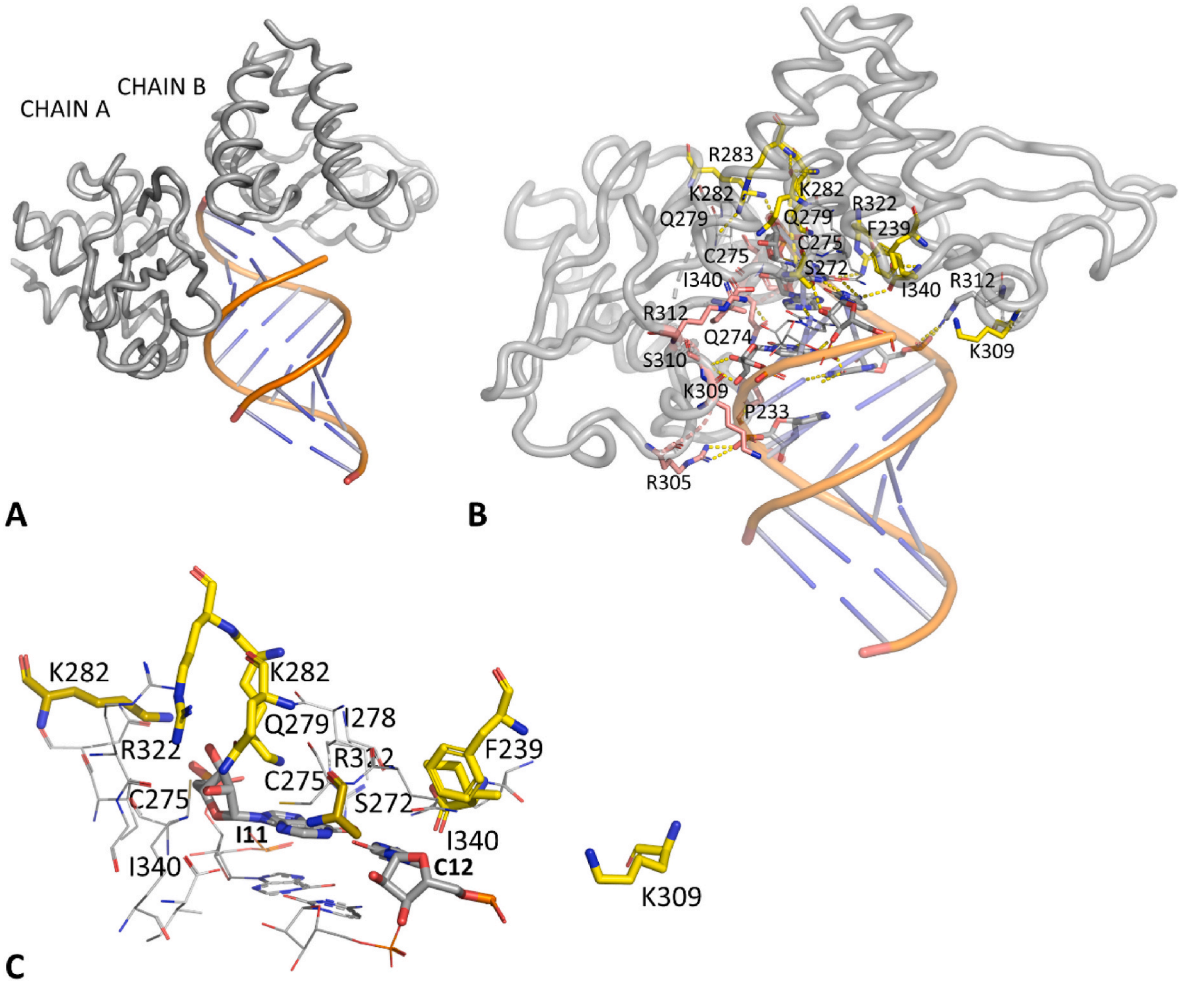

Fig. 3. Putative binding mode obtained through docking experiments of VP35 IID complexed with rintatolimod I:C terminal portion. A) VP35 dimer and dsRNA are represented as cartoons, respectively in grey and orange-light violet. B) The VP35 IID end-capping interacting residues are represented as yellow sticks and grey lines, while the backbone binding residues are highlighted in pink. The nucleotides are represented in light violet sticks. C) Close-up of end-capping interactions with terminal I_{11}:C_{12} base-pair.

number of conserved interacting residues may also help to avoid the problem of resistance.

3.2.2. Rintatolimod restoration of IFN-production in VP35 expressing HEK293T cells

The observed effects of rintatolimod on VP35 binding led us to investigate its ability of subverting VP35 inhibition of the IFN-production in an established cell-based method (Corona et al., 2022). In this system, human embryonic kidney HEK293 cells stably transfected with the SV40 large T antigen (HEK293T) are able to produce recombinant proteins whose genes are cloned into plasmid vectors containing the SV40 promoter. Hence, an empty vector (EV) or a vector expressing EBOV VP35 were transfected into HEK293T cells and the induction of luciferase under the control of IFN-I promoter was measured after stimulation by influenza virus dsRNA transfection (Cannas et al., 2015). Rintatolimod was able to significantly subvert the EBOV VP35 inhibition of the IFN production in a dose-dependent manner ($p = 0.009$ at 66 ng of transfected plasmid) (Fig. 4A).

Since in this system rintatolimod could potentially affect VP35 inhibition of IFN-I production acting either on the VP35-influenza virus dsRNA binding or/and boosting the IFN production, we asked whether rintatolimod could boost the influenza virus dsRNA induction of the IFN promoter activation in the same experimental conditions, using the EV as control. Results showed that when different rintatolimod concentrations were added to influenza virus dsRNA, rintatolimod was not able to boost IFN promoter activation (Fig. 4B), suggesting that in this system rintatolimod reverses IFN promoter activation mainly by sequestering VP35 and impeding it to bind to viral dsRNA without activating the RIG-1-like cytosolic helicases.

In order to confirm rintatolimod effects on restoring IFN production without boosting IFN-I production induced by viral dsRNA, we measured in the same cellular system the IFN gene expression by using RT-qPCR. In HEK293T cells our results demonstrate: i) rintatolimod alone was not able to induce a high transcription of IFN-β gene required to subvert VP35 inhibition (Fig. 5A left), ii) when transfected together with the viral dsRNA, rintatolimod did not boost IFN-β transcription but reduced its induction possibly by dose-dependently reducing the amount of viral dsRNA internalized through transfection (Fig. 5A right), and iii) when transfected together with the plasmid expressing EBOV VP35, rintatolimod, dose-dependently, significantly reverted VP35 inhibition of the IFN-β (Fig. 5B).

3.2.3. Restoration of TLR3 expression to TLR3 null cells and rintatolimod agonist activity essential for innate immune responses

Since it is established that HEK293T cells have low levels of TLRs (Hornung et al., 2002), the effect of rintatolimod on the VP35 inhibition of the IFN-β production in this cell line are probably due to its sequestration of VP35. In the mouse model, however, the mechanism through which rintatolimod led to survival of the infected mice was expected to involve also its ability to activate TLR3. In order to further explore this possibility, we used a HEK293 strain, termed HEK-Blue Null1, that completely lacks TLR3 expression, and HEK-Blue hTLR3 in which TLR-3 is stably expressed. Both cell lines have been bio-engineered to stably express the SEAP reporter gene under the control of the IFN-minimal promoter fused to five NF-κB and AP-1 binding sites. Stimulation of both cell lines with an NF-κB activator will induce the production of alkaline phosphatase quantified by substrate color production (see methods). Rintatolimod transfected into BlueTM Null1 cells was not able to induce IFN-β transcripts (Fig. 6A), while when transfected into HEK-Blue hTLR3 cells rintatolimod induced IFN-β transcripts in a dose-dependent manner (Fig. 6B). These results, on the one side confirmed what was previously observed, and suggested that rintatolimod can inhibit EBOV replication in the mouse model through a double mechanism as a dsRNA decoy for VP35 as well as its well established activity as a TLR3 agonist.

4. Discussion

dsRNA is a common component of viral replication, initiating systemic signaling cascades activating interferon (IFN) regulatory factors providing the antiviral activity of type I IFNs. The IFNs activate multiple IFN response pathways necessary to inhibit viral replication, including transitory expression of anti-viral enzymes such as 2′-5′-oligo-adenylate synthetase(Hartmann et al., 2003) and protein kinase R (Lemaire et al., 2008), which require dsRNA as a cofactor for activity. Highly virulent viruses (including EBOV) have evolved different strategies to block the biological activities associated with IFN induction and the subsequent multiplicity of IFN induced anti-viral responses and the initiation of adaptive immunity. VP35 is a multifunctional EBOV protein that is indispensable for replication as a component of the viral polymerase complex (Feldmann et al., 2013). Also known as the “lethal factor”, VP35 acts as an asymmetric homodimer (Ramaswamy et al., 2018) of A and B chains, which counteracts the host IFN innate immune response by blocking type I IFN transient gene activation (Prins et al., 2009). Key components of the innate immune response to viral infection include dsRNA activation of Toll-like receptor 3 (TLR3) and the RIG-1/mda5 cytosolic helicases (Zinzula and Tramontano, 2013). EBOV inhibition of these dsRNA responsive elements effectively disarms essential components of the innate immune response by binding replication associated viral dsRNAs. A positively charged 8 amino acid motif of the homologous VP35 dimer binds to the sequence-independent dsRNA phosphodiester backbone (Leung et al., 2010) resulting in the sequestration of viral dsRNA and resultant suppression of multiple steps in the IFN signaling cascade (Prins et al., 2009), which otherwise would lead to an antiviral state with activation of the initial rapid response innate arm and initiation of the subsequent long-term adaptive arm of the immune

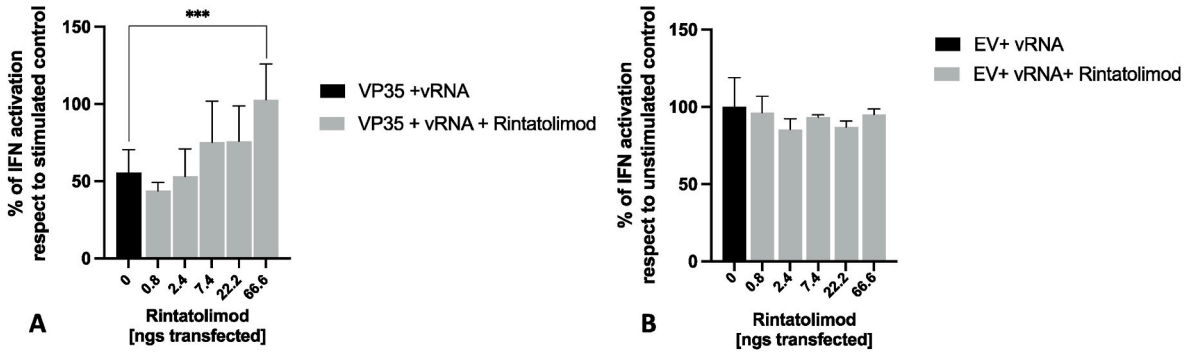

Fig. 4. Luciferase reporter gene assay for IFN promoter activation in HEK293T cells. A. Percentage of IFN promoter activation in presence of VP35 transfected as a function of transfected rintatolimod. B. Percentage of IFN promoter activation in presence of empty vector (pcDNA3) transfected as a function of transfected rintatolimod.

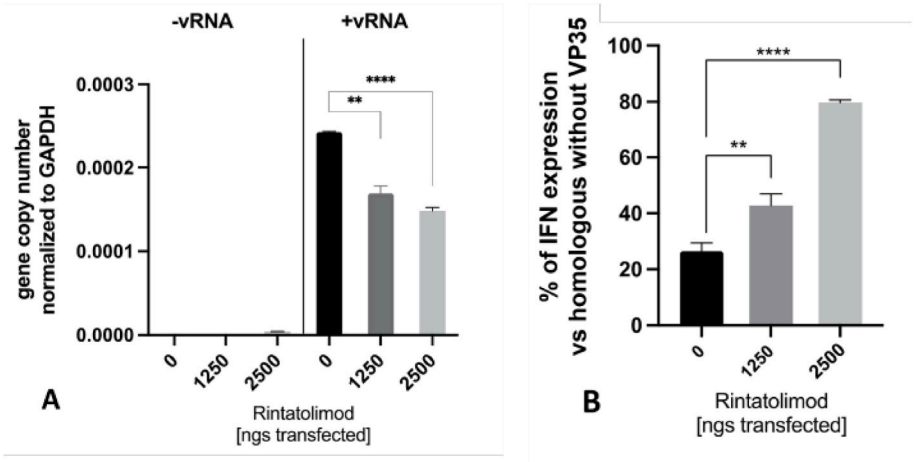

Fig. 5. RT-qPCR assay for IFN promoter activation in HEK293T. A. Rintatolimod effect on IFN-b minimal promoter activation in unstimulated (-vRNA) and stimulated conditions (+vRNA) (average of 2 experiments) based on gene copy number from rintatolimod effect on IFN-β expression in transfected empty vesicle (EV) stimulated or containing rintatolimod. B. % IFN-β expression as a function of rintatolimod in transfected VP35 cells. P value < 0.05 (*); p value < 0.01 (**); p value < 0.001 (***); p value < 0.0001 (****).

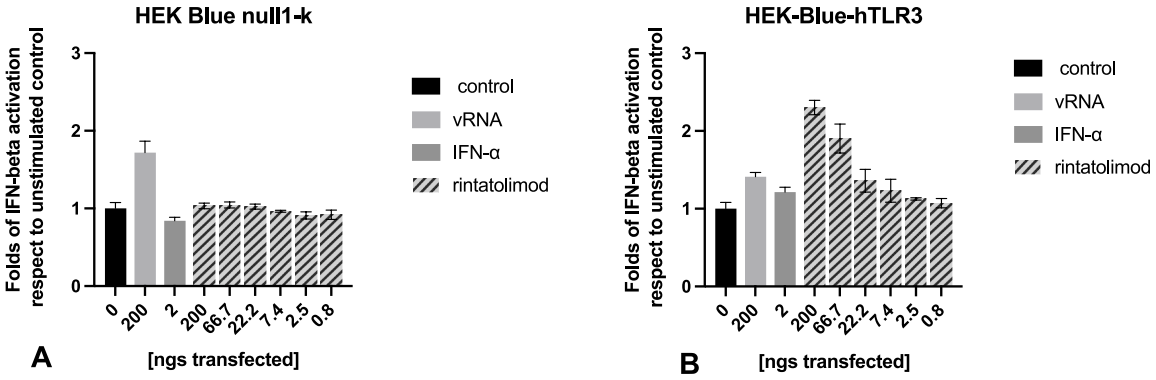

Fig. 6. HEK Blue IFN response agonist indicator PAMP (TLRs/Cytosolic helicases) cell system. A. HEK Blue null1-k cells. B. HEK-Blue-hTLR3 cells (stably HEK Blue null 1-k cells transfected human TLR3.

response. Our mode of action studies demonstrate that rintatolimod reduces VP35 dsRNA binding in the nanomolar range, reversing VP35 inhibition of the innate immune activation in cell-based systems in a dose dependent manner acting as a VP35 binding decoy and as a restricted TLR3 agonist.

Hence we sought to evaluate the putative binding mode of rintatolimod. ZDOCK is one of the best docking programs for predicting the structure of protein−protein complexes and protein-RNA complexes (Hwang et al., 2010a, 2010b; Pierce et al., 2011). The docking protocol was first validated and then applied to predict the terminal polyI:C rintatolimod binding mode with VP35 IID. The docking simulations highlighted the ability of polyI:C dsRNA to mimic the viral dsRNA thus preventing its binding.

These results are consistent with the experimental trials and provide some detail on the significant interactions and residues involved in the complex formation. It is also consistent with the dsRNA sequence-independent binding manner of VP35 IID and offers an interesting starting point for developing a new class of VP35 inhibitors.

We have demonstrated in this report, protection from death by EBOV-Zaire and its associated weight loss in a 100% lethal mouse model of EVD. More than 100,000 doses of rintatolimod have been administered to humans by the intravenous route in clinical trials and have been generally well tolerated (Mitchell, 2016). Systemic infused rintatolimod is rapidly eliminated from blood with a half-life of approximately 35 min (Mitchell, 2016). High MW molecules such as plasma proteins are rapidly absorbed by the peritoneal lymphatics upon IP administration and delivered to the systemic circulation (Regoeczi et al., 1989). In a recent review of IV versus IP routes in experimental animal studies, it was concluded that IP administration was justified as proof-of-concept (Shoyaib et al., 2019).

The 6 mg/kg doses used in the highly protective mouse model is easily achievable in humans (Supplementary Fig. 2). The data suggests that rintatolimod is a viable candidate to protect health care workers with high epidemic exposure to EBOV.

Declaration of competing interest

Authors AC, SD, GLD, AP, and EZ declare no conflict of interest. DS is the Medical Director of AIM ImmnunoTech. WMM is a member of Board of Directors for AIM ImmunoTech.

The funders had no role in the design of the study, in the collection, analyses, or interpretation of data, in the writing of the manuscript, or in the decision to publish the results.

Data availability

Data will be made available on request.

Acknowledgments

The authors thank Rekha Panchal and Veronica Soloveva for conducting under BSL4 protocols the EBOV cell culture and mouse challenge experiments at the US Army Medical Research Institute of Infectious Diseases (USAMRIID).A.C., S.D. and E.T thank Fondazione di

Sardegna FDS2019 EBOV CUPF72F20000270007 for financial support.

Appendix A. Supplementary data

Supplementary data to this article can be found online at https://doi.org/10.1016/j.antiviral.2023.105554.

References

Adasme, M.F., Linnemann, K.L., Bolz, S.N., Kaiser, F., Salentin, S., Haupt, V.J., Schroeder, M., 2021. PLIP 2021: expanding the scope of the protein–ligand interaction profiler to DNA and RNA. Nucleic Acids Res. 49 (W1), W530–W534. https://doi.org/10.1093/nar/gkab294.

Adepolu, P., 2021. Ebola returns to Guinea and DR Congo. Lancet 397, 781. https://doi:10.1016/S0140-6736(21)00506-7.

Bray, M., Davis, K., Geisbert, T., Schmaljohn, C., Huggins, J., 1998. A mouse model for evaluation of prophylaxis and therapy of Ebola hemorrhagic fever. J. Infect. Dis. 178, 651–661. https://doi.org/10.1086/515386.

Cannas, V., Daino, G.L., Corona, A., Esposito, F., Tramontano, E., 2015. A luciferase reporter gene assay to measure ebola virus viral protein 35-associated inhibition of double-stranded RNA-stimulated, retinoic acid-inducible gene 1-mediated induction of interferon β. J. Infect. Dis. 212, S277–S281. https://doi.org/10.1093/infdis/jiv214.

CDC, 2016. 2014-2016 ebola outbreak in West Africa. https://www.cdc.gov/vhf/ebola/history/2014-2016-outbreak/index.html. Accessed 1/2023.

Corona, A., Fanunza, E., Salata, C., Morwitzer, M.J., Distinto, S., Zinzula, L., Sanna, C., Frau, A., Daino, G.L., Quartu, M., et al., 2022. Cynarin blocks Ebola virus replication by counteracting VP35 inhibition of interferon-beta production. Antivir. Res. 198, 105251 https://doi.org/10.1016/j.antiviral.2022.105251.

Di Palma, F., Daino, G.L., Ramaswamy, V.K., Corona, A., Frau, A., Fanunza, E., Vargiu, A. V., Tramontano, E., Ruggerone, P., 2019. Relevance of Ebola virus VP35 homo-dimerization on the type I interferon cascade inhibition. Antivir. Chem. Chemother. 27, 1–13. https://doi.org/10.1177/2040206619889220.

Fanunza, E., Frau, A., Corona, A., Tramontano, E., 2019. Insights into ebola virus VP35 and VP24 interferon inhibitory functions and their initial exploitation as drug targets. Infect. Disord. - Drug Targets 19, 362–374. https://doi.org/10.2174/1871526519666181123145540.

Fanunza, E., Frau, A., Sgarbanti, M., Orsatti, R., Corona, A., Tramontano, E., 2018b. Development and validation of a novel dual luciferase reporter gene assay to quantify ebola virus VP24 inhibition of IFN signaling. Viruses 10, 98. https://doi.org/10.3390/v10020098.

Fanunza, E., Frau, A., Corona, A., Tramontano, E., 2018. Antiviral agents against ebola virus infection: repositioning old drugs and finding novel small molecules. Annu. Rep. Med. Chem. 251, 135–173. https://doi.org/10.1016/bs.armc.2018.08.004.

Feldmann, H., Sanchez, A., Geisbert, T.W., 2013. Filoviridae: marburg and ebola viruses. In: Fields Virology, sixth ed., (Vol 1. Wolters Kluwer Health Adis (ESP, pp. 923–956.

García-Sastre, A., 2017. Ten strategies of interferon evasion by viruses. Cell Host Microbe 22, 176–184. https://doi: 10.1016/j.chom.2017.07.012.

Gibb, T.R., Bray, M., Geisbert, T.W., Steele, K.E., Kell, W.M., Davis, K.J., Jaax, N.K., 2001. Pathogenesis of experimental Ebola Zaire virus infection in BALB/c mice. J. Comp. Pathol. 125, 233–242. https://doi.org/10.1053/jcpa.2001.0502.

Gowen, BB, Wong, MH, Jung, KH, Sanders, AB, Mitchell, WM, Alexopoulou, L, Flavell, RA, Sidwell, RW, 2007. TLR3 is essential for the induction of protective immunity against Punta Toro Virus infection by the double-stranded RNA (dsRNA), poly(I:C12U), but not Poly(I:C): differential recognition of synthetic dsRNA molecules. J Immunol 178, 5200–5208. https://doi.org/10.4049/jimmunol.178.8.5200.

Hartmann, R., Justesen, J., Sarkar, S.N., Sen, G.C., Yee, V.C., 2003. Crystal structure of the 2′-specific and double-stranded RNA-activated interferon-induced antiviral protein 2′-5′- oligoadenylate synthetase. Mol. Cell 12, 1173–1185. https://doi.org/10.1016/s1097-2765(03)00433-7.

Hornung, V., Rothenfusser, S., Britsch, S., Krug, A., Jahrsdörfer, B., Giese, T., Endres, S., Hartmann, G., 2002. Quantitative expression of toll-like receptor 1–10 mRNA in cellular subsets of human peripheral blood mononuclear cells and sensitivity to CpG oligodeoxynucleotides. J. Immunol. 168, 4531–4537. https://doi.org/10.4049/jimmunol.168.9.4531.

Hwang, H., Vreven, T., Pierce, B.G., Hung, J.H., Weng, Z., 2010a. Performance of ZDOCK and ZRANK in CAPRI rounds 13-19. Proteins: Struct., Funct., Bioinf. 78, 3104–3110. https://doi.org/10.1002/prot.22764.

Hwang, H., Vreven, T., Janin, J., Weng, Z., 2010b. Protein-protein docking benchmark version 4.0. Proteins: Struct., Funct., Bioinf. 78, 3111–3114. https://doi.org/10.1002/prot.22830.

Keita, A.K., Koundouno, F.R., Faye, M., Düx, A., Hinzmann, J., Diallo, H., Ayouba, A., Le Marcis, F., Soropogui, B., Ifono, K., Diagne, M.M., Sow, M.S., Bore, J.A., Calvignac-Spencer, S., Vidal, N., Camara, J., Keita, M.B., Renevey, A., Diallo, A., Soumah, A.K., Millimono, S.L., Mari-Saez, A., Diop, M., Doré, A., Soumah, F.Y., Kourouma, K., Vielle, N.J., Loucoubar, C., Camara, I., Kourouma, K., Annibaldis, G., Bah, A., Thielebein, A., Pahlmann, M., Pullan, S.T., Carroll, M.W., Quick, J., Formenty, P., Legand, A., Pietro, K., Wiley, M.R., Tordo, N., Peyrefitte, C., McCrone, J.T., Rambaut, A., Sidibé, Y., Barry, M.D., Kourouma, M., Saouromou, C.D., Condé, M., Baldé, M., Povogui, M., Keita, S., Diakite, M., Bah, M.S., Sidibe, A., Diakite, D., Sako, F.B., Traore, F.A., Ki-Zerbo, G.A., Lemey, P., Günther, S., Kafetzopoulou, L.E., Sall, A.A., Delaporte, E., Duraffour, S., Faye, O., Leendertz, F.H., Peeters, M., Toure, A., Magassouba, N.F., 2021. Resurgence of Ebola virus in 2021 in Guinea suggests a new paradigm for outbreaks. Nature 597, 539–543. https://doi.org/10.1038/s41586-021-03901-9.

Klosterman, P.S., Shah, S.A., Steitz, T.A., 1999. Crystal structures of two plasmid copy control related RNA duplexes: an 18 base pair duplex at 1.20 Å Resolution and a 19 base pair duplex at 1.55 Resolution. Biochemistry 38, 14784–14792. https://doi.org/10.1021/bi9912793.

Lemaire, P.A., Anderson, E., Lary, J., Cole, J.L., 2008. Mechanism of PKR activation by dsRNA. J. Mol. Biol. 381, 351–360. https://doi.org/10.1016/j.jmb.2008.05.056.

Leonard, J.N., Ghirlando, R., Askins, J., Bell, J.K., Margulies, D.H., Davies, D.R., Segal, D. M., 2008. The TLR3 signaling complex forms by cooperative receptor dimerization. Proc. Natl. Acad. Sci. U.S.A. 105, 258–263. https://doi.org/10.1073/pnas.0710779105.

Leung, D.W., Prins, K.C., Borek, D.M., Farahbakhsh, M., Tufariello, J.M., Ramanan, P., Nix, J.C., Helgeson, L.A., Otwinowski, Z., Honzatko, R.B., et al., 2010. Structural basis for dsRNA recognition and interferon antagonism by Ebola VP35. Nat. Struct. Mol. Biol. 17, 165–172. https://doi.org/10.1038/nsmb.1765.

Luo, J., Obmolova, G., Malia, T.J., Wu, S.J., Duffy, K.E., Marion, J.D., Bell, J.K., Ge, P., Zhou, Z.H., Teplyakov, A., et al., 2012. Lateral clustering of TLR3:dsRNA signaling units revealed by TLR3ecd:3Fabs quaternary structure. J. Mol. Biol. 421, 112–124. https://doi.org/10.1016/j.jmb.2012.05.006.

Mahanty, S., Bray, M., 2004. Pathogenesis of filoviral haemorrhagic fevers. Lancet Infect. Dis. 4, 487–498. https://doi.org/10.1016/s1473-3099(04)01103-x.

Mitchell, W.M., 2016. Efficacy of rintatolimod in the treatment of chronic fatigue syndrome/myalgic encephalomyelitis (CFS/ME). Expet Rev. Clin. Pharmacol. 9, 755–770. https://doi.org/10.1586/17512433.2016.1172960.

Mitchell, W.M., Nicodemus, C.F., Carter, W.A., Horvath, J.C., Strayer, D.R., 2014. Discordant biological and toxicological species responses to TLR3 activation. Am. J. Pathol. 184, 1062–1072. https://doi.org/10.1016/j.ajpath.2013.12.006.

Paulis, A.L., Corona, A., Tramontano, E., 2021. Inhibitors of Ebolavirus targeting innate immune evasion (Elsevier Inc.). Annu. Rep. Med. Chem. 57, 153–174. https://doi.org/10.1016/bs.armc.2021.09.003.

Pierce, B.G., Hourai, Y., Weng, Z., 2011. Accelerating protein docking in ZDOCK using an advanced 3D convolution library. PLoS One 6, e24657. https://doi.org/10.1371/journal.pone.0024657.

Pierce, B.G., Wiehe, K., Hwang, H., Kim, B.H., Vreven, T., Weng, Z., 2014. ZDOCK server: interactive docking prediction of protein-protein complexes and symmetric multimers. Bioinformatics 30, 1771–1773. https://doi.org/10.1093/bioinformatics/btu097.

Prins, K.C., Cárdenas, W.B., Basler, C.F., 2009. Ebola virus protein VP35 impairs the function of interferon regulatory factor-activating kinases IKKepsilon and TBK-1. J. Virol. 83, 3069–3077. https://doi.org/10.1128/jvi.01875-08.

Prins, K.C., Delpeut, S., Leung, D.W., Reynard, O., Volchkova, V.A., Reid, S.P., Ramanan, P., Cárdenas, W.B., Amarasinghe, G.K., Volchkov, V.E., et al., 2010. Mutations abrogating VP35 interaction with double-stranded RNA render Ebola virus avirulent in Guinea pigs. J. Virol. 84, 3004–3015. https://doi.org/10.1128/jvi.02459-09.

Ramaswamy, V.K., Di Palma, F., Vargiu, A., Corona, A., Piano, D., Ruggerone, P., Zinzula, L., Tramontano, E., 2018. Insights into the homo-oligomerization properties of N-terminal coiled-coil domain of Ebola virus VP35 protein. Virus Res. 247, 61–70. https://doi.org/10.1016/j.virusres.2018.02.003.

Regoeczi, E., Zaimi, O., Chindemi, P.A., Charlwood, P.A., 1989. Absorption of plasma proteins from peritoneal cavity of normal rats. Am. J. Physiol. 256, E447–E452. https://doi.org/10.1152/ajpendo.1989.256.4.e447.

Shoyaib, A.A., Archie, S.R., Karamyan, V.T., 2019. Intraperitoneal route of drug administration: should it Be used in experimental animal studies? Pharm. Res. (N. Y.) 23 (1), 12. https://doi.org/10.1007/s11095-019-2745-x, 37.

Seesuay, W., Jittavisutthikul, S., Sae-Lim, N., Sookrung, N., Sakolvaree, Y., Chaicumpa, W., 2018. Human transbodies that interfere with the functions of Ebola virus VP35 protein in genome replication and transcription and innate immune antagonism article. Emerg. Microb. Infect. 7, 41. https://doi.org/10.1038/s41426-018-0031-3.

Trumpfheller, C, Caskey, M, Nchinda, G, Longhi, MP, Mizenina, O, Huang, Y, Schlesinger, SJ, Colonna, M, Steinman, RM, 2008. The microbial mimic poly IC induces durable and protective CD4+ T cell immunity together with a dendritic cell targeted vaccine. Proc Natl Acad Sci USA 105, 2574–2579. https://doi.org/10.1073/pnas.0711976105.

WHO, 2023. Uganda declares end of Ebola disease outbreak, 1/2023. https://www.afro.who.int/countries/uganda/news/uganda-declares-end-ebola-disease-outbreak.

Woolsey, C., Menicucci, A.R., Cross, R.W., Luthra, P., Agans, K.N., Borisevich, V., Geisbert, J.B., Mire, C.E., Fenton, K.A., Jankeel, A., et al., 2019. A VP35 mutant ebola virus lacks virulence but can elicit protective immunity to wild-type virus challenge. Cell Rep. 28, 3032–3046.e6. https://doi.org/10.1016/j.celrep.2019.08.047.

Zinzula, L., Tramontano, E., 2013. Strategies of highly pathogenic RNA viruses to block dsRNA detection by RIG-I-like receptors: hide, mask, hit. Antivir. Res. 100, 615–635. https://doi.org/10.1016/j.antiviral.2013.10.002.

Zinzula, L., Esposito, F., Mühlberger, E., Trunschke, M., Conrad, D., Piano, D., Tramontano, E., 2009. Purification and functional characterization of the full length recombinant Ebola virus VP35 protein expressed in E. coli. Protein Expr. Purif 66, 113–119. https://doi.org/10.1016/j.pep.2009.02.008.

Zinzula, L., Esposito, F., Pala, D., Tramontano, E., 2012. DsRNA binding characterization of full length recombinant wild type and mutants Zaire ebolavirus VP35. Antivir. Res. 93, 354–363. https://doi.org/10.1016/j.antiviral.2012.01.005.

Zinzula, L., Nagy, I., Orsini, M., Weyher-Stingl, E., Bracher, A., Baumeister, W., 2019. Structures of ebola and reston virus VP35 oligomerization domains and comparative biophysical characterization in all ebolavirus species. Structure 27, 39–54.e6. https://doi.org/10.1016/j.str.2018.09.009.

Zinzula, L., Mereu, A.M., Orsini, M., Seeleitner, C., Bracher, A., Nagy, I., Baumeister, W., 2022. Ebola and Marburg virus VP35 coiled-coil validated as antiviral target by tripartite split-GFP complementation. iScience 25, 105354. https://doi.org/10.1016/j.isci.2022.105354.